Featured Article

Intravenous RNA Interference Gene Therapy Targeting the Human Epidermal Growth Factor Receptor Prolongs Survival in Intracranial Brain Cancer

Yun Zhang,[1] Yu-feng Zhang,[1] Joshua Bryant,[2] Andrew Charles,[2] Ruben J. Boado,[1,3] and William M. Pardridge[1]

Departments of [1]Medicine and [2]Neurology, University of California Los Angeles, Los Angeles, California and [3]Armagen Technologies, Inc., Santa Monica, California

ABSTRACT

Purpose: **The human epidermal growth factor receptor (EGFR) plays an oncogenic role in solid cancer, including brain cancer. The present study was designed to prolong survival in mice with intracranial human brain cancer with the weekly i.v. injection of nonviral gene therapy causing RNA interference (RNAi) of EGFR gene expression.**

Experimental Design: **Human U87 gliomas were implanted in the brain of adult scid mice, and weekly i.v. gene therapy was started at day 5 after implantation of 500,000 cells. An expression plasmid encoding a short hairpin RNA directed at nucleotides 2529–2557 within the human EGFR mRNA was encapsulated in pegylated immunoliposomes. The pegylated immunoliposome was targeted to brain cancer with 2 receptor-specific monoclonal antibodies (MAb), the murine 83–14 MAb to the human insulin receptor and the rat 8D3 MAb to the mouse transferrin receptor.**

Results: **In cultured glioma cells, the delivery of the RNAi expression plasmid resulted in a 95% suppression of EGFR function, based on measurement of thymidine incorporation or intracellular calcium signaling. Weekly i.v. RNAi gene therapy caused reduced tumor expression of immunoreactive EGFR and an 88% increase in survival time of mice with advanced intracranial brain cancer.**

Conclusions: **Weekly i.v. nonviral RNAi gene therapy directed against the human EGFR is a new therapeutic approach to silencing oncogenic genes in solid cancers. This is enabled with a nonviral gene transfer technology that delivers liposome-encapsulated plasmid DNA across cellular barriers with receptor-specific targeting ligands.**

Received 12/15/03; revised 2/13/04; accepted 2/25/04.

Grant support: Accelerate Brain Cancer Cure, Inc., NIH Grant R01-NS-39961, and NIH Grant R43-CA-109782.

The costs of publication of this article were defrayed in part by the payment of page charges. This article must therefore be hereby marked *advertisement* in accordance with 18 U.S.C. Section 1734 solely to indicate this fact.

Requests for reprints: William M. Pardridge, University of California Los Angeles, Warren Hall 13-164, 900 Veteran Avenue, Los Angeles, CA 90024. Phone: (310) 825-8858; Fax: (310) 206-5163; E-mail: wpardridge@mednet.ucla.edu.

INTRODUCTION

The human epidermal growth factor receptor (EGFR) plays an oncogenic role in 90% of primary brain cancers such as glioblastoma multiforme (1). In addition, the EGFR plays an oncogenic role in 70% of solid cancers that originate outside the brain (2). Because many solid cancers of peripheral organs metastasize to the brain, the EGFR plays a tumorigenic role in both primary brain cancer, as well as metastatic cancer to the brain. The development of brain cancer therapeutics, which knock-down the function of the EGFR, is made difficult by the presence of the blood-brain barrier (BBB). The BBB is formed by blood vessels that originate from normal brain, which perfuse the primary or metastatic cancer in brain. In the early and intermediate stages of brain cancer when therapeutic intervention is desirable, the capillaries perfusing the brain cancer have restrictive permeability properties (3), similar to capillaries in normal brain, which form the BBB (4). The problems presented by the BBB in the development of brain cancer therapeutics are illustrated in the case of Herceptin, a humanized monoclonal antibody to the HER2 receptor, which is a member of the *EGFR* gene family. Although Herceptin inhibits growth of HER2-positive cancer in the breast, this therapeutic is not effective against breast cancer that has metastasized to the brain (5). Large-molecule therapeutics, such as monoclonal antibodies or gene therapies, cannot cross the BBB.

Gene therapy of brain cancer offers the promise of specifically knocking down the expression of oncogenic genes such as *EGFR*. However, gene therapy is limited by the delivery problem, which is particularly difficult in brain because of the presence of the BBB. To circumvent the BBB, attempts have been made to deliver therapeutics to brain cancer by craniotomy. However, this approach is not effective, because there is limited diffusion of the therapeutic gene within the tumor from the *trans*-cranial injection site (6). Therapeutics can be delivered to all of the cells in brain cancer via the *trans*-vascular route across the BBB (4). The *trans*-vascular delivery of nonviral genes to brain is possible with a gene transfer technology that uses pegylated immunoliposomes (PILs; Ref. 7). With this approach, the nonviral plasmid DNA is encapsulated in the interior of an 85-nm anionic liposome, and the surface of the liposome is conjugated with several thousand strands of polyethylene glycol (PEG). This "PEGylation" process restricts uptake of the liposome by the reticuloendothelial system and enables a prolonged blood residence time (8). The PEGylated liposome is then targeted across biological barriers *in vivo* with receptor-specific peptidomimetic monoclonal antibodies (MAbs) as depicted in Fig. 1*A*. The application of the PIL nonviral gene transfer technology enabled a 100% increase in survival time of mice with intracranial human brain cancer with weekly i.v. injections of antisense gene therapy directed at the human EGFR (9). A eukaryotic expression plasmid, designated clone 882, which encodes for a 700 nucleotide RNA that is antisense to nucleo-

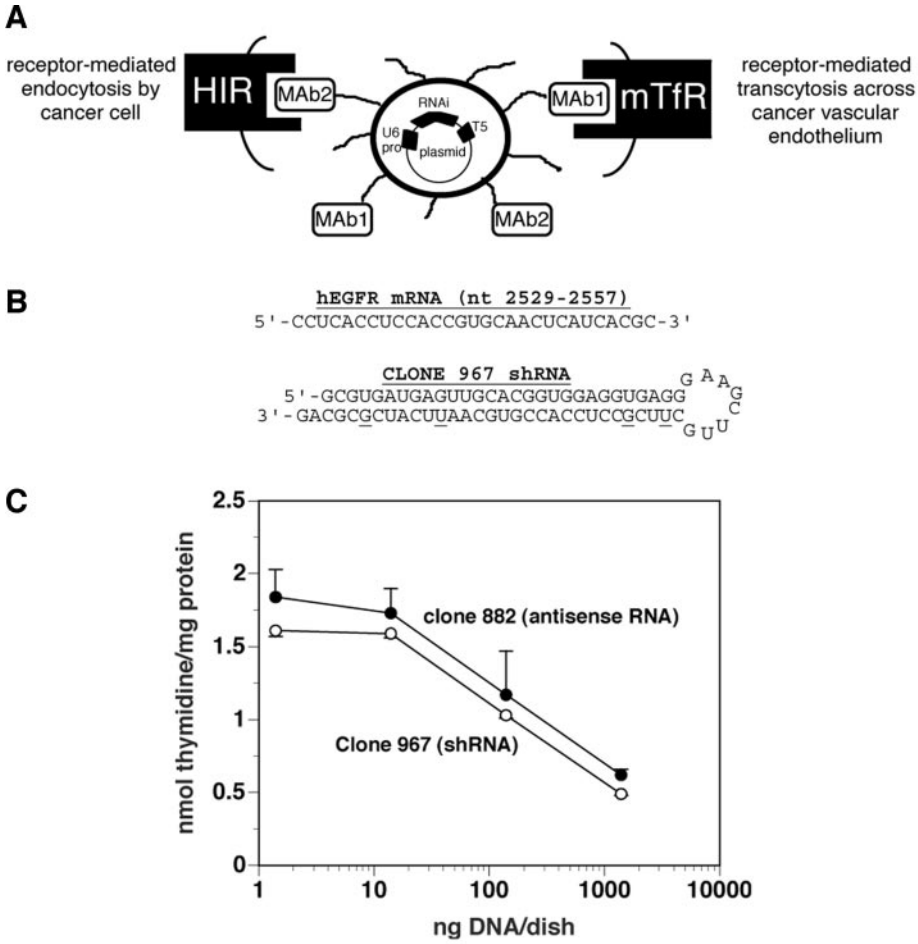

Fig. 1 Delivery of epidermal growth factor receptor RNA interference genes with pegylated immunoliposomes. *A*, model of pegylated immunoliposome (PIL) that is doubly targeted to both the mouse transferrin receptor (*mTfR*) with the 8D3 monoclonal antibody (*MAb1*) and to the human insulin receptor (*HIR*) with the 83–14 monoclonal antibody (*MAb2*). Encapsulated in the interior of the PIL is the plasmid DNA encoding the short hairpin RNA (*shRNA*), which produces the RNA interference (*RNAi*). The gene encoding the shRNA is driven by the U6 promoter (*pro*) and is followed on the 3′-end with the T5 termination sequence for the U6 RNA polymerase. *B*, nucleotide sequence of the human epidermal growth factor receptor (*hEGFR*) sequence between nucleotides 2529 and 2557 is shown on *top*. The sequence and secondary structure of the shRNA produced by clone 967 is shown on the *bottom*. The antisense strand is 5′ to the 8 nucleotide loop, and the sense strand is 3′ to the loop. The sense strand contains 4 G/U mismatches to reduce the Tm of hybridization of the stem loop structure; the sequence of the antisense strand is 100% complementary to the target mRNA sequence. *C*, human U87 glioma cells were incubated with [^{3}H]thymidine for a 48 h period that follows a 5-day period of incubation of the cells with HIRMAb-targeted PILs carrying either clone 967 or 882 plasmid DNA. A dose of 1.4, 14, 140, or 1400 ng plasmid DNA per dish was used in each experiment. Data are mean ($n = 3$ dishes); *bars*, ±SE.

tides 2317–3006 of the human EGFR (10), was encapsulated in PILs that were doubly targeted to brain cancer *in vivo* with 2 MAbs of different receptor specificities (9). One MAb, the rat 8D3 MAb to the mouse transferrin receptor (TfR), enabled transport of the PIL across the mouse BBB forming the microvasculature of the intracranial cancer. A second MAb targeted the human insulin receptor (HIR) that was expressed on the human brain cancer plasma membrane (Fig. 1*A*). The targeting MAbs act as molecular Trojan horses to ferry the PIL across membrane barriers, and these MAbs are species specific (7). The 8D3 to the mouse TfR enables transport across the first barrier, the mouse BBB, but does not mediate transport of the PIL across the second barrier, the human brain cancer cell membrane. This is accomplished with the HIRMAb, which does not react with the mouse vascular endothelial insulin receptor. The doubly conjugated PIL is designated HIRMAb/TfRMAb-PIL (Fig. 1*A*). To augment the potency of the clone 882 expression plasmid, this vector contained the oriP and Epstein-Barr nuclear antigen (EBNA)-1 elements (10), which allow for a single round of replication of the expression plasmid with each division of the cancer cell (11). The inclusion of the oriP/EBNA-1 elements within the expression plasmid enables a 10-fold increase in the level of gene expression in human U87 glioma cells (12). However, the *EBNA-1* gene encodes a tumorigenic *trans*-acting factor (13), and this formulation may not be desirable in human gene therapy. It is possible that the EBNA-1 element would not be required if a more potent form of antisense gene therapy were used.

RNA interference (RNAi) is a new form of antisense gene therapy wherein an expression plasmid encodes for a short hairpin RNA (shRNA) that is composed of a stem-loop structure (14). This shRNA is processed in the cell to an RNA duplex with a 3′-overhang, and this short RNA duplex mediates RNAi or post-transcriptional gene silencing. Although RNAi-based gene therapy offers promise for the treatment of cancer, the limiting factor is delivery. Therefore, the present studies were designed to test the therapeutic efficacy of i.v. RNAi-based gene therapy directed at the human EGFR in mice with brain cancer. A new expression plasmid was designed, which lacked the oriP/EBNA-1 elements and which encoded for an shRNA directed at a specific sequence in the human EGFR mRNA, and this plasmid was incorporated in HIRMAb/TfRMAb-PILs. These PILs were administered i.v. on a weekly schedule to mice with intracranial human brain cancer.

MATERIALS AND METHODS

Materials. 1-Palmitoyl-2-oleoyl-*sn*-glycerol-3-phosphocholine and dimethyldioctadecylammonium bromide were purchased from Avanti-Polar Lipids, Inc. (Alabaster, AL). Distearoylphosphatidylethanolamine-PEG^{2000} was obtained from Shearwater Polymers (Huntsville, AL), where PEG^{2000} is 2000 Dalton polyethyleneglycol. Distearoylphosphatidylethanolamine-PEG^{2000}-maleimide was custom synthesized by Shearwater Polymers. [α-^{32}P]dCTP (3000 Ci/mmol) was from Perkin-Elmer (Boston, MA), and *N*-succinimidyl[2,3-^{3}H]propionate (101 Ci/mmol) and protein G Sepharose CL-4B were purchased from Amersham-Pharmacia Biotech (Arlington Heights, IL). The 2-iminothiolane (Traut's reagent) and bicinchoninic acid protein assay reagents were obtained from Pierce Chemical Co. (Rockford, IL). The anti-TfRMAb used in this study is the 8D3 rat MAb to the mouse TfR (15). The 8D3 MAb is specific for the mouse TfR and is not active in human cells. The anti-insulin receptor MAb used for gene targeting to human cells is the murine 83–14 MAb to the human insulin receptor (HIR; Ref. 16). The TfRMAb and HIRMAb were individually purified with protein G affinity chromatography from hybridoma generated ascites. Custom olideoxynucleotides (ODNs) were obtained from Biosource (Camarillo, CA). The nick translation system and the *Escheria coli* DH5α competent cells were purchased from Invitrogen (San Diego, CA). All of the restriction endonucleases were obtained from New England Biolabs (Boston, MA). Horse serum, rabbit serum, donkey serum, mouse IgG1 isotype, rat IgG, and glycerol-gelatin were from Sigma-Aldrich Chemical Co. (St. Louis, MO). The biotinylated horse antimouse IgG, biotinylated rabbit antirat IgG, Vectastain ABC kit, 3-amino-9-ethylcarbazole substrate kit, and Vectashield mounting medium were purchased from Vector Laboratories (Burlingame, CA); 488 Alexa fluor donkey antimouse IgG and 594 Alexa fluor donkey antirat IgG were obtained from Molecular Probes (Eugene, OR). OCT compound (Tissue-Tek) was purchased from Sakura FineTek (Torrance, CA).

Construction of Expression Plasmids. ODN duplexes corresponding to the various EGFR shRNAs were designed as described by Paddison *et al.* (17), and shown in Table 1. The shRNA sequence intentionally included nucleotide mismatches in the sense strand (Fig. 1*B*) to reduce the formation of DNA hairpins during cloning. Because the antisense strand remains unaltered, these G-U substitutions do not interfere with the RNAi effect (18). Forward ODNs contain a U6 polymerase stop signal (T_6; Table 1). Reverse ODNs contain 4-nucleotide overhangs specific for the *Eco*RI and *Apa*I restriction sites at 5′- and 3′-end, respectively (Table 1), to direct subcloning into the cohesive ends of the expression plasmid (19). The empty expression plasmid is designated clone 959 (Table 2). Complementary ODNs were heat denatured (4 min at 94°C) and annealed at 65°C for 16 h in 10 mM sodium phosphate (pH = 7.4), 150 mM sodium chloride, and 1 mM EDTA. Double-stranded ODNs were ligated into the expression plasmid at *Eco*RI and *Apa*I sites. *E. coli* DH5α competent cells were transformed, and clones with the correct RNAi inserts were confirmed by DNA sequencing using the T3 primer and restriction endonuclease mapping with *Nae*I.

A total of 6 anti-EGFR shRNA encoding expression plasmids were produced and designated clones 962–964 and 966–968 (Tables 1–2). The sequence of the antisense strand of each of the 6 shRNAs matches 100% with the target sequence of the human EGFR (accession no. X00588). The EGFR knockdown potency of these 6 shRNA encoding expression plasmids was compared with the EGFR knockdown effect of clone 882, which is a eukaryotic expression plasmid described previously (10). Clone 882 is derived from pCEP4, is driven by the SV40 promoter, contains EBNA-1/oriP elements, and encodes for a 700 nucleotide antisense RNA complementary to nucleotides 2317–3006 of the human EGFR (10). The RNAi effect on the human EGFR was screened by measuring the rate of [^{3}H]thymidine incorporation into human U87 glioma cells in tissue culture.

Thymidine Incorporation in U87 Glioma Cells. U87 human glioma cells were grown in six-well cluster dishes with MEM containing 10% fetal bovine serum. After the cells reached 50–60% confluence, the growth medium was replaced with 1.5 ml of serum-free MEM containing 1 μg of each plasmid DNA (clone 959, 962–964, 966–968, or 882) and 10 μl (20 μg) of' Lipofectamine and incubated for 4 h at 37°C. The medium was replaced with MEM with 10% fetal bovine serum and incubated for 24 h. A final concentration of 2 μCi/ml of [^{3}H]thymidine and 10 μM of unlabeled thymidine were added to each dish, and dishes were incubated at 37 C for 48 h. The cells were harvested for measurement of [^{3}H]thymidine incorporation as described previously (10).

The transfection of the U87 cells with Lipofectamine demonstrated that clone 967 was the most potent clone causing RNAi of EGFR expression. A dose response study with clone 967 was performed, in parallel with a dose response study for clone 882, which encodes for the 700 nucleotide EGFR antisense RNA (10). U87 cells were grown on 35-mm collagen-treated dishes. After the cells reached 50–60% confluence, the medium was aspirated, and 2 ml of fresh MEM with 10% fetal bovine serum and HIRMAb-PILs encapsulated with clone 967 or clone 882 at a dose of 1.4, 0.14, 0.014, or 0.0014 μg DNA/dish were added. The cells were incubated for 5 days at 37°C. During this period, 2 ml of fresh medium was added after 3 days of incubation. At 5 days, the medium was aspirated, and 2 ml of fresh growth medium containing 2 μCi/ml of [^{3}H]thymidine and 10 μM of unlabeled thymidine were added to each

Table 1 Design of shRNA[a] to target EGFR mRNA: list of ODNs used for the construction of expression plasmids

Nucleotide overhangs to the *Eco*RI and *Apa*I restriction sites at 5′- and 3′-end of reverse ODNs are underlined. EGFR mRNA nucleotide sequences are taken from accession no. X00588.

Plasmid number	EGFR mRNA (nt)		ODN sequence
962	187–219	Forward:	GCTGCCCCGGCCGTCCCGGAGGGTCGCATGAAGCTTGATGCGACTCTTCGGGACGGTCGGGGTAGCGCTTTTTT
		Reverse:	AATTAAAAAAGCGCTACCCCGACCGTCCCGAAGAGTCGCATCAAGCTTCATGCGACCCTCCGGGACGGCCGG GGCAGCGGCC
963	2087–2119	Forward:	GATCTTAGGCCCATTCGTTGGACAGCCTTGAAGCTTGAGGGTTGTCCGACGAATGGGCCTAAGATTCCTTTTTT
		Reverse:	AATTAAAAAAGGAATCTTAGGCCCATTCGTCGGACAACCCTCAAGCTTCAAGGCTGTCCAACGAATGGGCCT AAGATCGGCC
964	3683–3715	Forward:	GTCCTGCTGGTAGTCAGGGTTGTCCAGGCGAAGCTTGGTCTGGATAATCCTGACTATCAGCAGGACTTTTTTTT
		Reverse:	AATTAAAAAAAAGTCCTGCTGATAGTCAGGATTATCCAGACCAAGCTTCGCCTGGACAACCCTGACTACCAGC AGGACGGCC
966	2346–2374	Forward:	GTCCCTTATACACCGTGCCGAACGCACCGGAAGCTTGCGGTGCGTTCGGCGCGGTGTGTGAGGGATTCTTTTTT
		Reverse:	AATTAAAAAAGAATCCCTCACACACCGCGCCGAACGCACCGCAAGCTTCCGGTGCGTTCGGCACGGTGTATAA GGGACGGCC
967	2529–2557	Forward:	GCGTGATGAGTTGCACGGTGGAGGTGAGGGAAGCTTGCTTCGCCTCCACCGTGCAATTCATCGCGCAGTTTTTT
		Reverse:	AATTAAAAAACTGCGCGATGAATTGCACGGTGGAGGCGAAGCAAGCTTCCCTCACCTCCACCGTGCAACTCAT CACGCGGCC
968	2937–2965	Forward:	GGATGGAGGAGATCTCGCTGGCAGGGATTGAAGCTTGAGTCTCTGCCGGCGAGATCTCCTCCGTCCTGTTTTTT
		Reverse:	AATTAAAAAACAGGACGGAGGAGATCTCGCCGGCAGAGACTCAAGCTTCAATCCCTGCCAGCGAGATCTCCT CCATCCGGCC

[a] shRNA, short hairpin RNA; EGFR, epidermal growth factor receptor; ODN, olideoxynucleotide; nt, nucleotide.

dish, followed by a 48-h incubation at 37°C. At the end of the incubation, [^{3}H]thymidine incorporation was measured and expressed as nmol thymidine incorporated/mg cell protein, as described previously (10).

EGFR Western Blotting. Human U87 cells were grown in 35-mm dishes to 80% confluency and then exposed for 4 h to serum-free medium containing 1.5 μg/dish clone 967, 962, 952, or 882 in Lipofectamine, as described previously (10). Clones 962 and 967 produce an anti-EGFR shRNA clone (Tables 1–2), clone 882 produces a 700 nucleotide RNA antisense to the human EGFR mRNA (10), and clone 952 produces an shRNA directed against the luciferase mRNA, as described previously (19). After the initial 4-h incubation, the medium was replaced with fresh medium containing 10% fetal bovine serum, and the cells were harvested 48 h later for electrophoresis through a reducing 7.5% SDS-PAGE and blotting to nitrocellulose. The primary antibody was a 1:1000 dilution of the rabbit polyclonal antibody (#2232) to the human EGFR from Cell Signaling Technology (Beverly, MA). The secondary antibody was a conjugate of peroxidase and a goat-antirabbit antibody from Sigma (A0545), and the immune reaction was determined with the enhanced chemiluminescence method as described previously (10). The X-ray film was scanned into Adobe PhotoShop and intensity of the band corresponding to the 170 kDa immunoreactive EGFR was quantified with NIH Image software.

Synthesis of PILs. Clone 967 or 882 plasmid DNA was encapsulated in PILs as described previously (8, 10, 20). The liposome was 85–100 nm in diameter, and the surface of the liposome was conjugated with several thousand strands of 2000 Da PEG. The tips of about 1–2% of the PEG strands were conjugated with 83–14 HIRMAb and the 8D3 TfRMAb, as described previously (9). Any plasmid DNA not encapsulated in the interior of the liposome was quantitatively removed by exhaustive nuclease treatment (8). In a typical synthesis, 30–40% of the initial plasmid DNA (200 μg) was encapsulated within 20 μmol of lipid, and each liposome had a range of 43–87 MAb molecules conjugated to the PEG strands (9).

Calcium Signaling. U87 cells were grown in 35-mm plastic flasks and passaged onto 18-mm diameter glass coverslips in 12-well plates. Growth medium was composed of DMEM-F12 supplemented with 5% fetal bovine serum, 5% horse serum, penicillin, and streptomycin. Cells were grown at 37° in a humidified incubator with 5% CO_2. At 1–2 days after passage, cells were exposed to HIRMAb-PILs carrying clone 967 plasmid DNA by addition of the PILs directly to the wells

Table 2 shRNA[a] target site within human EGFR mRNA and biological activity in U87 cells

Human U87 glioma cells were incubated with 1 μg plasmid DNA and 20 μg Lipofectamine in serum-free medium for 4 h. The medium was then replaced, and 24 h later [^{3}H]thymidine (2 μCi/ml) and 10 μM unlabeled thymidine were added, and the cells were incubated for a 48-h period before measurement of thymidine incorporation. Data are mean ± SE (n = 3 dishes).

Plasmid number	RNA type	EGFR mRNA sequence	Thymidine incorporation (% inhibition)[b]
959	None	None	0
962	shRNA	187–219	0
963	shRNA	2087–2119	0
966	shRNA	2346–2374	59 ± 1
967	shRNA	2529–2557	97 ± 3
968	shRNA	2937–2965	72 ± 3
964	shRNA	3683–3715	59 ± 3
882	Antisense	2317–3006	100

[a] shRNA, short hairpin RNA; EGFR, epidermal growth factor receptor.

[b] % inhibition of thymidine incorporation = [(A − B)/(A − C)] ×100, where A = thymidine incorporation with clone 959 (the empty expression plasmid), B = thymidine incorporation with clone 962, 963, 964, 966, 967, or 968, and C = thymidine incorporation with clone 882.

without medium exchange. Cells were maintained in the same medium (with or without PILs) for 12–48 h before experimentation. Epidermal growth factor (EGF) has been shown to evoke intracellular calcium signaling in brain tumor cells (21), and a similar response in human U87 glioma cells was found in these studies. Changes in $[Ca^{2+}]_i$ were measured using a video imaging system as described previously (22). Cells were incubated at room temperature for 30 min - 1 h in HBSS containing 2.5 μM fluo-4-AM (Molecular Probes). Cells were then washed and maintained in fresh medium for at least 30 min to allow complete de-esterification of dye. Cells were then placed in an open slide flow-chamber on the stage of a Nikon inverted microscope. Changes in $[Ca^{2+}]_i$ in fields of cells (typically 60–80 cells/field) were measured with 488-nm excitation via a Nikon ×20 epifluorescence objective. Fluorescence at 510 nm was recorded with a silicon-intensified tube camera (Hamamatsu) and digitized at a resolution of 640 × 480 pixels using an Axon Image Lightning board and Image WorkBench software. Spontaneous activity was recorded for 60–120 min, after which EGF (200 ng/ml in HBSS) was applied by bath perfusion. The change in fluorescence of fluo-4 for individual cells in the field was displayed as a continuous record showing the time course of change in fluorescence for regions of interest drawn for each individual cell. A response to EGF, ATP, or bradykinin was defined as an increase in fluo-4 fluorescence of at least 20% above baseline during 120 s of EGF exposure.

***In Vivo* Brain Cancer Model.** All of the animal procedures were approved by the University of California Los Angeles Animal Research Committee. Female severe combined immunodeficient (scid) mice weighing 19–21 g were purchased from the Jackson Laboratory (Bar Harbor, ME). A burr hole was drilled 2.5 mm to the right of midline and 1 mm anterior to bregma. U87 glioma cells were suspended in serum-free MEM containing 1.2% methylcellulose. Five μl of cell suspension (5×10^5 cells) were injected into the right caudate-putamen nucleus at a depth of 3.5 mm over 2 min, using a 10-μl Hamilton syringe with fixed needle. The animals were treated i.v. once a week starting at day 5 after implantation. By 5 days after the implantation of 500,000 U87 cells, the tumor is large and fills the entire volume of the striatum in brain (23). Weekly i.v. gene therapy was administered at 5, 12, 19, and 26 days after implantation. Mice were treated with either saline or 5 μg/mouse of clone 967 DNA encapsulated in the HIRMAb/TfRMAb-PILs.

Confocal Microscopy and Immunocytochemistry. Brains were removed immediately after sacrifice and cut into coronal slabs from the center of tumor. Slabs were embedded in OCT medium and frozen in dry ice powder. Frozen sections (20 μm) of mouse brain were cut on a Mikron HM505E cryostat. Sections were fixed in cold 100% methanol for 20 min at −20°C. For confocal microscopy, nonspecific binding of proteins was blocked with 10% donkey serum-PBS for 30 min. The sections were incubated in primary antibody overnight at 4°C. The primary antibodies were the rat 8D3 MAb to the mouse TfR (10 μg/ml) and the mouse 528 MAb against the human EGFR (10 μg/ml). After a PBS wash, a rhodamine-conjugated donkey antirat IgG secondary antibody, 5 μg/ml, was added for 30 min at room temperature. The slides were then washed and incubated with fluorescein-conjugated goat antimouse IgG at 5 μg/ml for 30 min at room temperature. The sections were mounted on slides, and viewed with a ×4X objective and a Zeiss LSM 5 PASCAL confocal microscope with dual argon and helium/neon lasers. The sample was scanned in multitrack mode to avoid leakage of the fluorescein signal into the rhodamine channel. Sections were scanned at intervals of 0.8 μm and reconstructed with Zeiss LSM software. Control experiments used either a rat IgG (Sigma) or a mouse IgG1 (Sigma) as primary antibodies in lieu of the rat antimouse TfR or the mouse antihuman EGFR antibody, respectively.

Immunocytochemistry was performed by the avidin-biotin complex immunoperoxidase method (Vector Laboratories). To stain the human EGFR, the mouse 528 MAb antihuman EGFR was used as the primary antibody (24); to stain the mouse TfR, the rat 8D3 MAb antimouse TfR was used as the primary antibody (9). Endogenous peroxidase was blocked with 0.3% H_2O_2 in 0.3% horse serum-PBS for 30 min; nonspecific binding of proteins was blocked with 3% horse or rabbit serum in PBS for 30 min. For mouse TfR staining using rat 8D3 MAb, rabbit serum was used in the blocking steps. Sections were then incubated in 10 μg/ml of primary antibody overnight at 4°C. Identical concentrations of isotype control antibody were also used as primary antibody. Mouse IgG1 was used as the isotype antibody for 528 MAb, and rat IgG was used as the isotype control antibody for 8D3 MAb. After incubation and wash in PBS, sections were incubated in either biotinylated horse antimouse IgG (for 528 MAb) or biotinylated rabbit antirat IgG (for 8D3 MAb) for 30 min, before color development with 3-amino-9-ethylcarbazole. Slides were not counterstained. The sections immunostained with the mouse vascular specific marker, the TfRMAb, were quantified with light microscopy and an optical grid and expressed as capillaries per 0.1 mm^2 of brain tissue.

RESULTS

Design of shRNA Encoding Plasmid. Forward and reverse synthetic ODNs were designed to produce shRNAs directed at three broadly spaced regions of the human EGFR mRNA at nucleotides 187–219 (clone 962), 2087–2119 (clone 963), and 3683–3715 (clone 964), and the ODN sequences are given in Table 1. The biological activity of the EGFR RNAi plasmids was tested by measuring the inhibition of [^{3}H]thymidine incorporation in U87 human glioma cells (Table 2). Clones 962–963 caused no knockdown of EGFR action, and the effect of clone 964 was intermediate (Table 2). Therefore, a second series of ODNs were designed to produce shRNAs directed at three different regions within nucleotides 2300–3000 of the human EGFR mRNA, including 2346–2374 (clone 966), 2529–2557 (clone 967), and 2937–2965 (clone 968) as shown in Table 1. Whereas the knockdown of EGFR function was intermediate with clones 966 and 968, clone 967 produced a level of inhibition of [^{3}H]thymidine incorporation comparable with clone 882 (Table 2). The sequence and secondary structure of the shRNA produced by clone 967 is shown in Fig. 1*B*.

The anti-EGFR shRNA encoding plasmids were initially delivered to U87 human glioma cells with Lipofectamine (Table 2). Clone 967 or 882 plasmid DNA were then encapsulated in HIRMAb-targeted PILs and added to U87 cells without Lipofectamine at various doses of plasmid DNA ranging from 1.4 to

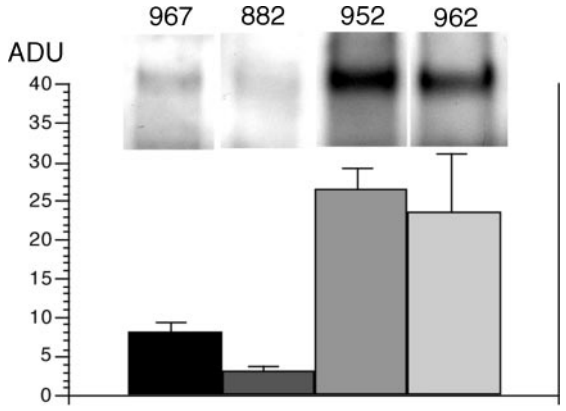

Fig. 2 Epidermal growth factor receptor Western blotting. U87 human glioma cells were exposed to clone 967, clone 882, clone 952, or clone 962 plasmid DNA for 48 h and harvested for epidermal growth factor receptor Western blotting. Films were scanned and quantified with NIH Image software; arbitrary densitometric units (*ADU*) were computed for each treatment group. A representative scan is shown at the top of each mean (n = 3–4 dishes); *bars*, ±SE.

1400 ng/dish. Either plasmid DNA was equally active in suppressing thymidine incorporation with an ED_{50} of ~100 ng/dish (Fig. 1*C*).

Western Blotting. The EGFR Western blots are shown in Fig. 2, as are the results of the scanning densitometry of the intensity of the 170 kDa EGFR band (Fig. 2, top). There is no significant difference in the level of the immunoreactive EGFR in the cells expose to either clone 952, which produces an shRNA directed against luciferase (19), or clone 962, which produces an shRNA against an inactive site of the EGFR mRNA (Table 2). However, exposure of the cells to either clone 967 or clone 882 caused a 68% and 88% inhibition of the expression of the immunoreactive EGFR, respectively (Fig. 2).

Calcium Signaling in U87 Glioma Cells in Tissue Culture. To confirm the inhibition of functional EGFR expression by PIL-mediated RNAi in cell culture, we examined Ca^{2+} signaling in U87 cells in response to EGF using fluorescence video microscopy. The majority of U87 cells respond to EGF (200 ng/ml) with an increase in $[Ca^{2+}]_i$ that begins 10–30 s after exposure to EGF and continues for 60–300 s (Table 3; Fig. 3*A*). Treatment of U87 cells with HIRMAb-PILs containing 0.125 μg clone 967 plasmid DNA per 18 mm coverslip resulted in a significant reduction in the number of cells responding to EGF, whereas treatment with 0.25–1.5 μg DNA of clone 967 abolished the Ca^{2+} response to EGF in nearly all of the cells (Table 3; Fig. 3*B*). The inhibition of the response to EGF was observed at 12 and 24 h after exposure to the PILs, whereas the Ca^{2+} signaling response was largely restored at 48 h after PIL exposure (Table 3). To determine whether the PILs or shRNA encoding plasmid DNA had any nonspecific effects on Ca^{2+} signaling, we examined the response of the cells to ATP and bradykinin. The percentage of cells responding to ATP (1 μM) and bradykinin (100 nM) were not significantly different for controls *versus* cells exposed to HIRMAb-targeted PILs encapsulated with clone 967 plasmid DNA (1.5 μg) for 24 h (Table 3). The amplitude and duration of the Ca^{2+} responses were also similar, indicating that the treatment did not have a nonspecific effect on Ca^{2+} signaling evoked by other ligands.

Intravenous Anti-EGFR Gene Therapy of Intracranial Brain Cancer. Human U87 glioma cells were implanted in the caudate-putamen nucleus of adult scid mice, which causes death at 14–20 days secondary to the growth of large intracranial tumors. Starting on day 5 after implantation, mice were treated with weekly i.v. injections of either saline or 5 μg/mouse of clone 967 plasmid DNA encapsulated in PILs that were doubly targeted with both the 83–14 murine MAb to the HIR and the 8D3 rat MAb to the mouse TfR (Fig. 1*A*). The saline-treated mice died between 14 and 20 days after implantation with an ED_{50} of 17 days (Fig. 4). The mice treated with i.v. gene therapy died between 31 and 34 days postimplanation with an ED_{50} of 32 days, which represents an 88% increase over the ED_{50} in the saline-treated animals (Fig. 4).

The tumors were examined at autopsy by immunocytochemistry using the rat 8D3 MAb to the mouse TfR, which stains the vessels perfusing the tumor (Fig. 5). Unlike the cancer cells, the cells comprising the tumor vessels are of mouse brain origin and express the murine TfR (9). The tumors from the saline-treated animals were well vascularized and expressed the murine TfR (Fig. 5, *A–C*). Fig. 5*B* shows the immunoreactive murine TfR on the vascular endothelium of normal brain and the tumor. A blood vessel originating from normal brain and extending into the tumor is visible (see asterisk, Fig. 5*B*). The border between the tumor and the normal brain frequently had a low vascular density as shown in Fig. 5*B*. The vascular density in the tumors of the mice treated with clone 967 encapsulated in the HIRMAb/TfRMAb-PIL was visibly reduced (Fig. 5*D*), although gene therapy did not cause a visible decrease in vascular density in normal brain as shown in Fig. 5*E*. The vascular density in the tumor center, the tumor periphery, and the con-

Table 3 Effect of EGFR[a] RNAi on intracellular calcium flux in human U87 glioma cells

Signaling molecule	RNAi dose (μg DNA/dish)	Exposure time (hr)	$[Ca^{++}]i$ response (% of cells)	Cells counted
EGF (200 ng/ml)	0	–	90 ± 6	360
	0.125	24	21 ± 8[b]	180
	0.25	24	12 ± 3[b]	180
	0.5	24	4 ± 2[b]	180
	1.0	24	4 ± 3[b]	180
	1.5	24	6 ± 4[b]	180
EGF (200 ng/ml)	0	–	91 ± 5	180
	1.5	12	5 ± 3[b]	180
	1.5	24	6 ± 4[b]	180
	1.5	48	63 ± 4[c]	180
ATP (1 μM)	0	–	67 ± 8	180
	1.5	24	72 ± 6	180
BK (100 nM)	0	–	94 ± 2	180
	1.5	24	94 ± 3	180

[a] EGFR, epidermal growth factor receptor; RNAi, RNA interference; EGF, epidermal growth factor; BK, bradykinin

[b] $P < 0.005$ difference from control, which is the RNAi dose = 0. Mean ± SE.

[c] $P < 0.05$ difference from control, which is the RNAi dose = 0. Mean ± SE.

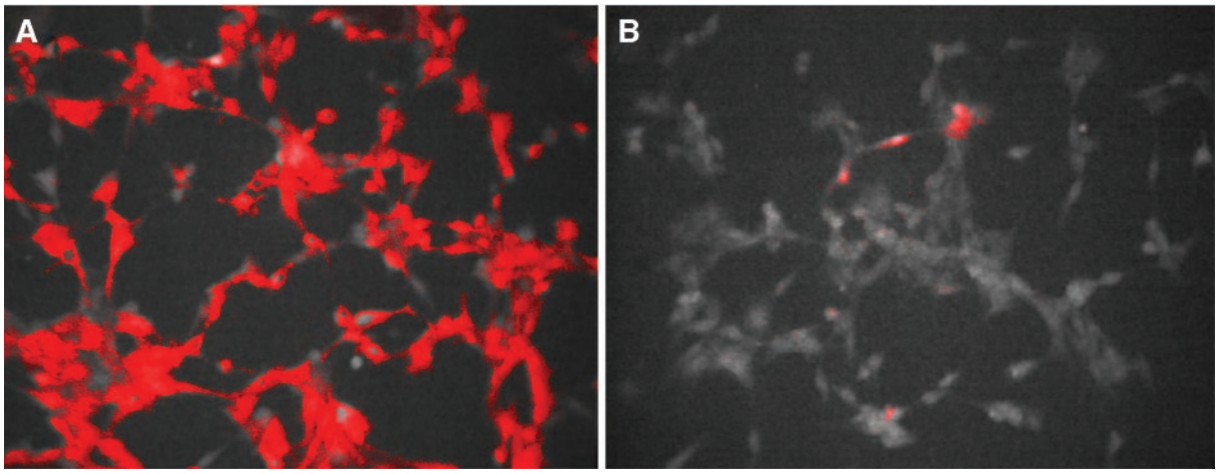

Fig. 3 Knock down of epidermal growth factor receptor-mediated calcium signaling by RNA interference. Maximum Fluo-4 fluorescence in cultured U87 human glioma cells is shown after stimulation with 200 ng/ml human epidermal growth factor. Before measurement of calcium-induced fluorescence, the cells were preincubated for 24 h with either vehicle (*A*) or HIRMAb-targeted pegylated immunoliposomes carrying clone 967 plasmid DNA at a dose of 0.5 μg DNA per dish (*B*).

tralateral normal brain was quantified by light microscopy. Although gene therapy caused no decrease in the vascular density of normal brain, the treatment with clone 967 resulted in an 80% and 72% decrease in vascular density in the tumor center and tumor periphery, respectively, as compared with the saline-treated animals (Table 4).

Confocal Microscopy. The tumor sections were immunostained with both the rat 8D3 MAb to the vascular mouse TfR (red channel) and the murine 528 MAb to the tumor EGFR (green channel) as shown in Fig. 6. There is down-regulation of the immunoreactive EGFR in the RNAi-treated tumors (Fig. 6, *A–C*) relative to the saline treated tumors (Fig. 6, *D–F*).

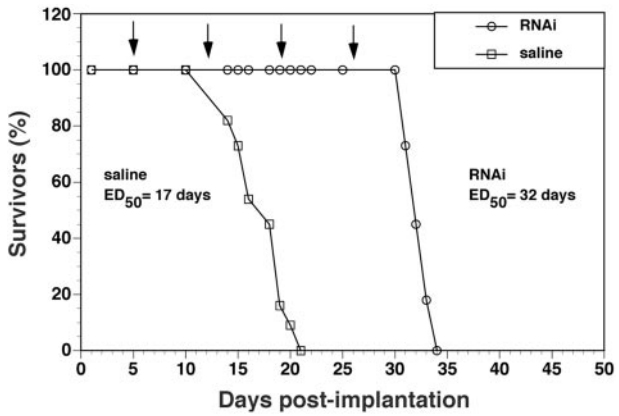

Fig. 4 Survival study. i.v. RNA interference (RNAi) gene therapy directed at the human epidermal growth factor receptor is initiated at 5 days after implantation of 500,000 U87 cells in the caudate putamen nucleus of scid mice, and weekly i.v. gene therapy is repeated at days 12, 19, and 26 (*arrows*). The control group was treated with saline on the same days. There are 11 mice in each of the two treatment groups. The time at which 50% of the mice were dead (ED_{50}) is 17 days and 32 days in the saline and RNAi groups, respectively. The RNAi gene therapy produces an 88% increase in survival time, which is significant at the $P < 0.005$ level (Fisher's exact test).

DISCUSSION

The results of these studies are consistent with the following conclusions. First, it is possible to knock down *EGFR* gene expression with i.v. gene therapy that uses expression plasmids encoding a shRNA directed at nucleotides 2529–2557 of the human EGFR mRNA (Table 2). Second, EGFR expression knockdown is demonstrated by the inhibition of thymidine incorporation or calcium flux in human U87 glioma cells in tissue culture (Tables 2 and 3; Fig. 3), by the decrease in the expression of immunoreactive EGFR in cell culture (Fig. 2), and by the decrease in brain cancer expression of immunoreactive EGFR *in vivo* (Fig. 6). Third, anti-EGFR gene therapy has an antiangiogenic effect and results in a 72–80% decrease in vascular density of the tumor (Fig. 5; Table 4). Fourth, weekly i.v. anti-EGFR gene therapy results in an 88% increase in survival time in adult mice with intracranial brain cancer (Fig. 4).

The discovery of RNAi-active target sequences within the human EGFR transcript required several iterations (Tables 1 and 2). These findings were consistent with the suggestion of McManus and Sharp (14), that ~1 of 5 target sequences yield therapeutic effects in RNAi. Prior work had shown that *EGFR* gene expression could be inhibited with RNA duplexes delivered to cultured cells with oligofectamine (25). The present studies demonstrate that *EGFR* gene expression can be inhibited with shRNA expression plasmids. The effect of shRNA expression plasmids on EGFR gene expression was screened with thymidine incorporation assays (Table 2), because the EGFR mediates thymidine incorporation into EGFR-dependent cells (26). The thymidine incorporation assays were confirmed by Western blotting, which showed that clones 967 and 882 knock down the EGFR (Fig. 2). In contrast, clone 962, which has no effect on thymidine incorporation into U87 cells, also has no effect on the expression of the immunoreactive EGFR (Fig. 2).

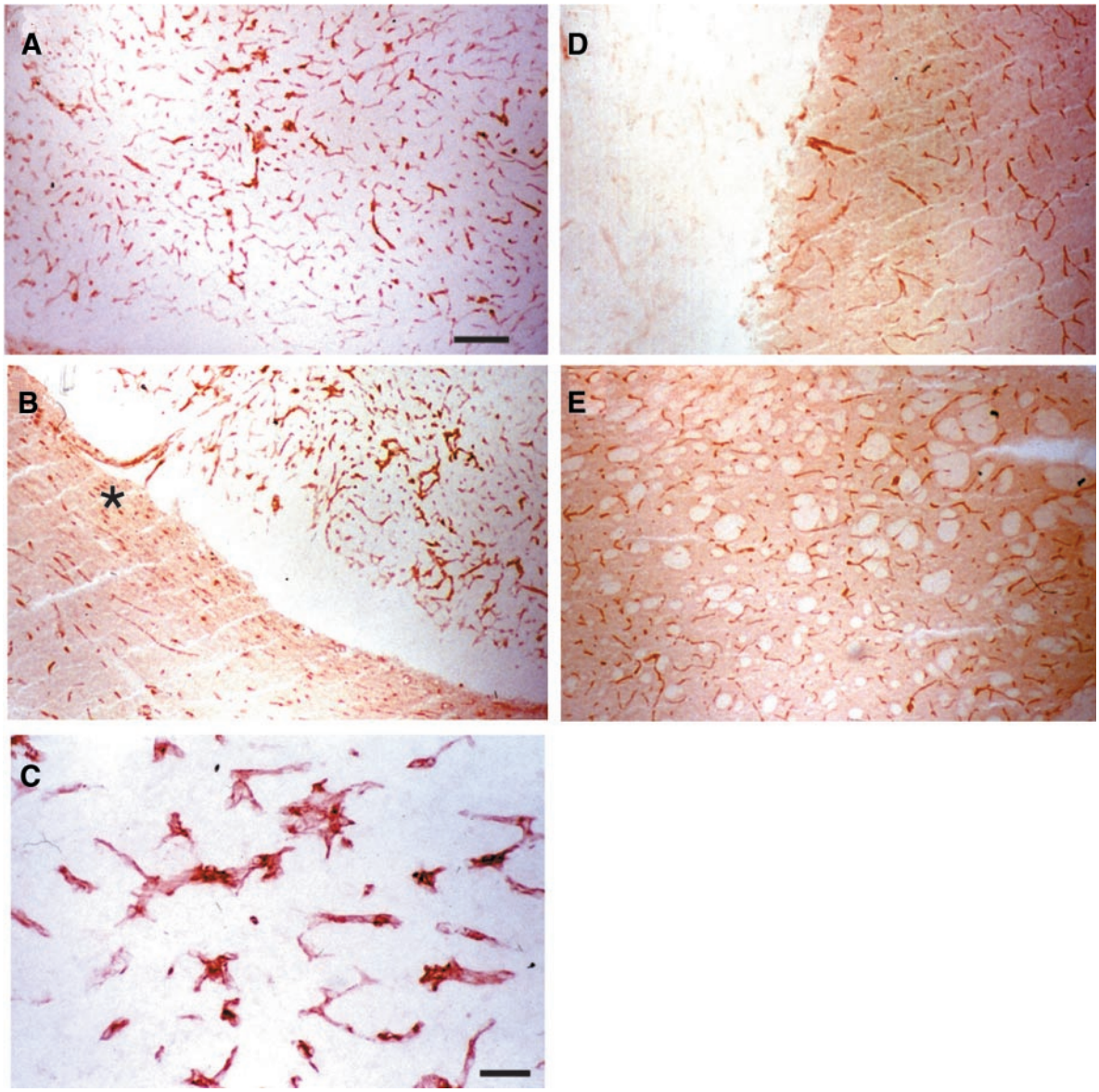

Fig. 5 Immunocytochemistry. Mouse brain autopsy sections are stained with either the rat 8D3 monoclonal antibody to the mouse transferrin receptor (*A–E*) or control rat IgG (not shown). No sections are counterstained. The magnification in panels *A, B, D,* and *E* is the same, and the magnification bar in *A* is 135 μm. The magnification bar in *C* is 34 μm. *A–C* are sections taken from the brain of the saline treated mice, and *D–E* are sections of brain taken from mice treated with the clone 967 gene therapy. *A–C* show the density of the tumor vasculature in the saline treated mice. *B* shows a section containing normal brain at the *bottom* of the panel and tumor at the *top* of the panel; the tumor is vascularized by a vessel originating from normal brain (marked by ∗ in *B*). *D* shows the tumor on the *left* of the panel and normal brain on the *right* of the panel; this section is taken from a mouse treated with RNA interference (RNAi) gene therapy and illustrates the decreased vascular density in the RNAi-treated animals. The vascular density of normal brain is not changed in the RNAi-treated animals as shown in *E*. The control rat IgG primary antibody gave no reaction with mouse brain and the sections are not counterstained or shown.

Similarly, clone 952, which produces an antiluciferase shRNA (19), has no effect on the EGFR (Fig. 2). On the basis of the cell culture work evaluating thymidine incorporation (Table 2) and Western blotting (Fig. 2), clone 967 was chosen for additional evaluation of RNAi-based gene therapy to knock down human *EGFR* gene expression. Clone 967 produces an shRNA directed against nucleotides 2529–2557 (Fig. 1*B*), and this target sequence is within the 700 nucleotide region of the human EGFR mRNA that is targeted by antisense RNA expressed by clone 882 (10). Clone 967 and clone 882 equally inhibit thymidine incorporation in human U87 cells (Table 2), and this is evidence for the increased potency of RNAi-based forms of antisense gene therapy. The clone 882 plasmid contains the EBNA-1/oriP gene element (10), which enables a 10-fold increase in expression of the *trans*-gene in cultured U87 cells (12). Therefore, the increased potency of the RNAi approach to antisense gene

Table 4 Capillary density in brain tumor and normal brain

Mean ± SE (n = 15 fields analyzed from 3 mice in each of the treatment groups).

Region	Treatment	Capillary density per 0.1 mm^2
Tumor center	Saline	15 ± 2
	RNAi	3 ± 0
Tumor periphery	Saline	29 ± 4
	RNAi	8 ± 1
Normal brain	Saline	35 ± 1
	RNAi	33 ± 1

therapy enabled the elimination of the potentially tumorigenic EBNA-1 element in the expression plasmid.

Clone 967 was delivered to cultured U87 cells with HIRMAb-targeted PILs, and this resulted in a 95% knockdown of EGFR functionality based on measurements of EGFR-induced calcium fluxes (Fig. 3*B;* Table 3). The RNAi effect of clone 967 was specific to the EGFR, as the PIL delivery of this plasmid to the U87 cells had no effect on ATP- or bradykinin-mediated calcium fluxes in the cells (Table 3). Clone 967 knocked down EGFR function in a dose-dependent mechanism, with respect to inhibition of both calcium flux (Table 3) and thymidine incorporation (Fig. 1*C*) with an ED_{50} of ~100 ng plasmid DNA/dish.

Suppression of the EGFR by clone 967 encapsulated in the HIRMAb/TfRMAb-PILs is also demonstrated *in vivo*, as the confocal microscopy shows a down-regulation of the immunoreactive EGFR (Fig. 6, *A–C*). Other evidence for the suppression of the EGFR in the tumor *in vivo* is the 72–80% reduction in tumor vascular density in the tumors of mice treated with anti-EGFR gene therapy as compared with the vascular density of brain tumors in mice treated with saline (Table 4). The EGFR has a proangiogenic function in cancer (27). The results of the present study show that suppression of EGFR function in brain tumors results in a reduction in vascularization of the tumor (Table 4). The reduction in tumor vascular density is not a nonspecific effect of PIL administration, because there is no reduction in vascular density in control mouse brain (Table 4). A Blast analysis of nucleotide sequences of the human EGFR mRNA (accession no. X00588) and the mouse EGFR mRNA (accession no. AF275367) shows there is only 76% identity in the mouse sequence corresponding to 2529–2557 of the human EGFR. Therefore, the shRNA produced by clone 967 would not be expected to effect endogenous mouse EGFR expression.

The present studies show an 88% increase in survival time with weekly i.v. gene therapy using clone 967 encapsulated in

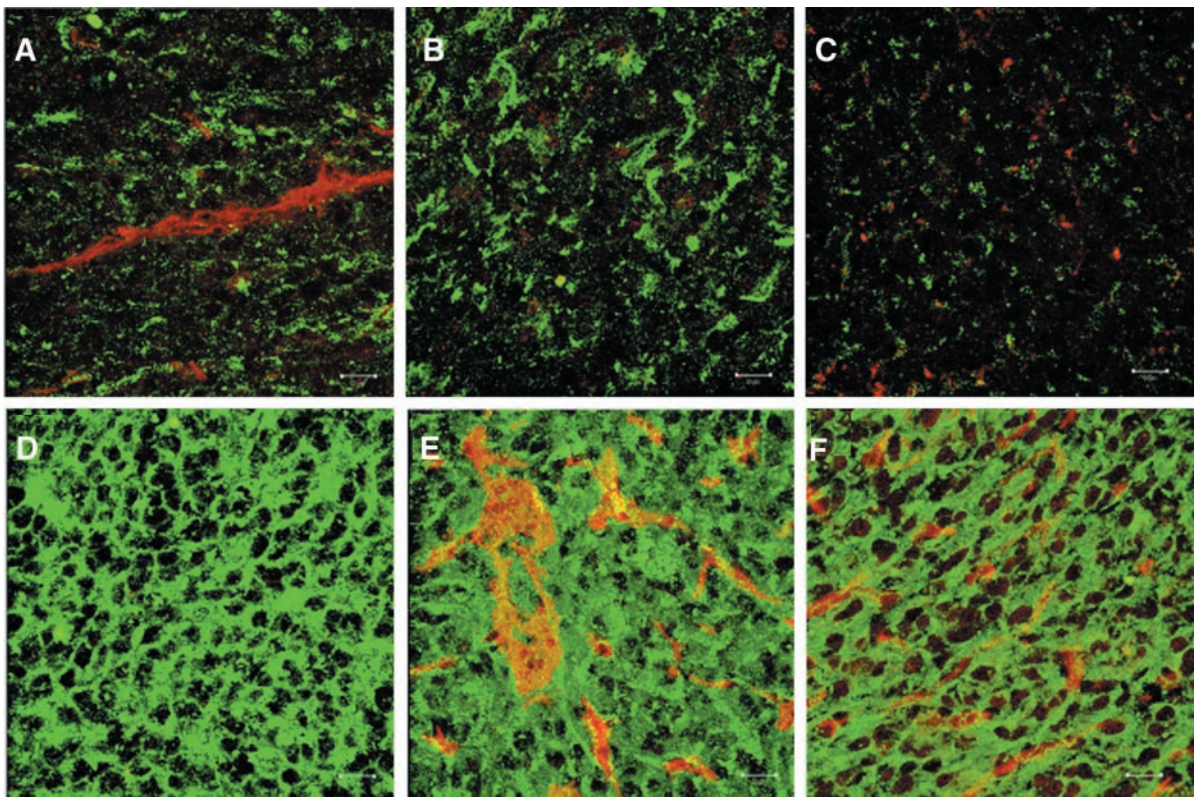

Fig. 6 Knock down of brain tumor epidermal growth factor receptor (EGFR) by RNA interference (RNAi). Confocal microscopy of intracranial glioma. Sections are shown for brain tumors from RNAi-treated mice (*A–C*) or saline-treated mice (*D–F*). The sections are doubly labeled with the murine 528 monoclonal antibody to the EGFR (*green*) and the rat 8D3 monoclonal antibody to the mouse transferrin receptor (*red*). There is decreased immunoreactive EGFR in the tumor cells in the RNAi-treated mice (*A–C*) relative to the saline treated mice (*D–F*). The saline treated animals died at 14–15 days after implantation (*D–F*), whereas the RNAi-treated animals died at 31 days (*A*), 33 days (*B*), and 34 days (*C*) after implantation, respectively, which was 5, 7, and 8 days after the last dose of i.v. RNAi gene therapy (Fig. 4).

HIRMAb/TfRMAb-PILs (Fig. 4). This increase in survival time is not a nonspecific effect of PIL administration, because prior work has shown no change in survival with the weekly administration of PILs carrying a luciferase expression plasmid (9). The increase in survival obtained with weekly i.v. anti-EGFR gene therapy is comparable with the prolongation of survival time in mice treated with high daily doses of the EGFR-tyrosine kinase inhibitor, ZD1839 (Iressa; Ref. 28). However, Iressa was not effective in the treatment of brain cancer expressing mutant forms of the EGFR (28). Many primary and metastatic brain cancers express mutations of the human EGFR (29, 30), and it is possible to design RNAi-based gene therapy that will knock down both wild-type and mutant EGFR mRNAs.

In summary, the present studies demonstrate that weekly i.v. RNAi gene therapy directed against the human EGFR causes an 88% increase in survival time in adult mice with intracranial human brain cancer. The high therapeutic efficacy of the PIL gene transfer technology is possible, because this approach delivers therapeutic genes to brain via the *trans*-vascular route (4). The PIL nonviral gene transfer technology could be used to simultaneously knock down tumorigenic genes and to replace mutated tumor suppressor genes in brain cancer. The efficacy of the PIL nonviral gene transfer technology has been demonstrated in primates, and levels of gene expression in primate brain are 50-fold greater than comparable levels of gene expression in rodent brain (31). PILs carrying therapeutic genes can be delivered to human brain cancer using genetically engineered MAbs. A chimeric HIRMAb (32) has the same activity in terms of binding to the human BBB *in vitro*, or transport across the primate BBB *in vivo*, as the original murine HIRMAb used in these studies. Future clinical applications of the PIL approach to gene therapy of brain cancer should enable targeting of the therapeutic gene to the cancer cell with minimal general toxicity. Weekly administration of PILs has no toxic effects and causes no inflammation in brain (33). With regard to eliminating ectopic expression of the exogenous gene in noncancer cells, prior work has shown that region-specific gene expression is possible with tissue-specific gene promoters in either mice (34) or primates (35). It may be possible to restrict therapeutic gene expression to the cancer cell by putting the gene under the influence of a promoter taken from a gene selectively expressed in brain cancer. Alternatively, many solid cancers express mutant forms of the EGFR, which are produced from aberrantly processed mRNAs that contain nucleotide sequences not found in normal cells (36). These sequences can be used as shRNA targets to selectively knock down mutant transcripts in cancer cells.

REFERENCES

1. Kuan CT, Wikstrand CJ, Bigner DD. EGF mutant receptor vIII as a molecular target in cancer therapy. Endocr Relat Cancer 2001;8:83–96.

2. Nicholson, RI, Gee, JM, Harper, ME. EGFR and cancer prognosis. Eur J Cancer 2001;37(Suppl 4):S9–15.

3. Zhang RD, Price JE, Fujimaki T, Bucana CD, Fidler IJ. Differential permeability of the blood-brain barrier in experimental brain metastases produced by human neoplasms implanted into nude mice. Am J Pathol 1992;141:1115–24.

4. Pardridge WM. Drug and gene delivery to the brain: the vascular route. Neuron 2002;36:555–8.

5. Bendell JC, Domchek SM, Burstein HJ, et al. Central nervous system metastases in women who receive trastuzumab-based therapy for metastatic breast carcinoma. Cancer 2003;97:2972–7.

6. Ram Z, Culver KW, Oshiro EM, et al. Therapy of malignant brain tumors by intratumoral implantation of retroviral vector-producing cells. Nat Med 1997;3:1354–61.

7. Pardridge WM. Drug and gene targeting to the brain with molecular Trojan horses. Nat Rev Drug Discov 2002;1:131–9.

8. Shi N, Pardridge WM. Non-invasive gene targeting to the brain. Proc Natl Acad Sci USA 2000;97:7567–72.

9. Zhang Y, Zhu C, Pardridge WM. Antisense gene therapy of brain cancer with an artificial virus gene delivery system. Mol Ther 2002;6:67–72.

10. Zhang Y, Lee HJ, Boado RJ, Pardridge WM. Receptor-mediated delivery of an antisense gene to human brain cancer cells. J Gene Med 2002;4:183–94.

11. Makrides SC. Components of vectors for gene transfer and expression in mammalian cells. Protein Expr Purif 1999;17:183–202.

12. Zhang Y, Boado RJ, Pardridge WM. Marked enhancement in gene expression by targeting the human insulin receptor. J Gene Med 2003;5:157–63.

13. Snudden DK, Smith PR, Lai D, Ng MH, Griffin BE. Alterations in the structure of the EBV nuclear antigen, EBNA1, in epithelial cell tumours. Oncogene 1995;10:1545–52.

14. McManus MT, Sharp PA. Gene silencing in mammals by small interfering RNAs. Nat Rev Genet 2002;3:737–47.

15. Lee HJ, Engelhardt B, Lesley J, Bickel U, Pardridge WM. Targeting rat anti-mouse transferrin receptor monoclonal antibodies through the blood-brain barrier in the mouse. J Pharmacol Exp Ther 2000;292:1048–52.

16. Pardridge WM, Kang Y-S, Buciak JL, Yang J. Human insulin receptor monoclonal antibody undergoes high affinity binding to human brain capillaries in vitro and rapid transcytosis through the blood-brain barrier in vivo in the primate. Pharm Res 1995;12:807–16.

17. Paddison P, Caudy A, Bernstein E, Hannon G, Conklin D. Short hairpin RNAs (shRNAs) induce sequence-specific silencing in mammalian cells. Genes Dev 2002;16:948–58.

18. Yu JY, Taylor J, DeRuiter SL, Vojtek AB, Turner DL. Simultaneous inhibition of GSK3α and GSK3β using hairpin siRNA expression vectors. Mol Ther 2003;7:228–36.

19. Zhang Y, Boado RJ, Pardridge WM. In vivo knockdown of gene expression in brain cancer with intravenous RNAi in adult rats. J Gene Med 2003;5:1039–45.

20. Pardridge WM. Gene targeting in vivo with pegylated immunoliposomes. Methods Enzymol 2003;373:507–28.

21. Hernandez M, Barrero MJ, Crespo MS, Nieto ML. Lysophosphatidic acid inhibits Ca^{2+} signaling in response to epidermal growth factor receptor stimulation in human astrocytoma cells by a mechanism involving phospholipase C_{γ} and a $G_{\alpha i}$ protein. J Neurochem 2000;75:1575–82.

22. Stout CE, Costantin JL, Naus CC, Charles AC. Intercellular calcium signaling in astrocytes via ATP release through connexin hemichannels. J Biol Chem 2002;277:10482–8.

23. Lal S, Lacroix M, Tofilon P, Fuller GN, Sawaya R, Lang FF. An implantable guide-screw system for brain tumor studies in small animals. J Neurosurg 2002;92:326–33.

24. Kurihara A, Pardridge WM. Imaging brain tumors by targeting peptide radiopharmaceuticals through the blood-brain barrier. Canc Res 1999;54:6159–63.

25. Nagy P, Arndt-Jovin DJ, Jovin TM. Small interfering RNAs suppress the expression of endogenous and GFP-fused epidermal growth factor receptor (erbB1) and induce apoptosis in erbB1-overexpressing cells. Exp Cell Res 2003;285:39–49.

26. Ewald JA, Coker KJ, Price JO, Staros JV, Guyer CA. Stimulation of mitogenic pathways through kinase-impaired mutants of the epidermal growth factor receptor. Exp Cell Res 2001;268:262–73.

27. Abe T, Terada K, Wakimoto H, et al. PTEN decreases in vivo vascularization of experimental gliomas in spite of proangiogenic stimuli. Cancer Res 2003;63:2300–5.

28. Heimberger AB, Learn CA, Archer GE, et al. Brain tumors in mice are susceptible to blockade of epidermal growth factor receptor (EGFR) with the oral, specific, EGFR-tyrosine kinase inhibitor ZD1839 (iressa). Clin Cancer Res 2002;8:3496–502.

29. Luwor RB, Johns TG, Murone C, et al. Monoclonal antibody 806 inhibits the growth of tumor xenografts expressing either the de2–7 or amplified epidermal growth factor receptor (EGFR) but not wild-type EGFR. Cancer Res 2001;61:5355–61.

30. Lal A, Glazer CA, Martinson HM, et al. Mutant epidermal growth factor receptor up-regulates molecular effectors of tumor invasion. Cancer Res 2002;62:3335–9.

31. Zhang Y, Schlachetzki F, Pardridge WM. Global non-viral gene transfer to the primate brain following intravenous administration. Mol Ther 2003;7:11–8.

32. Coloma MJ, Lee HJ, Kurihara A, et al. Transport across the primate blood-brain barrier of a genetically engineered chimeric monoclonal antibody to the human insulin receptor. Pharm Res 2000;17:266–74.

33. Zhang Y-F, Boado RJ, Pardridge WM. Absence of toxicity of chronic weekly intravenous gene therapy with pegylated immunoliposomes. Pharm Res 2003;20:1779–85.

34. Shi N, Zhang Y, Boado RJ, Zhu C, Pardridge WM. Brain-specific expression of an exogenous gene after i.v. adminstration. Proc Natl Acad Sci USA 2001;98:12754–9.

35. Zhang Y, Schlachetzki F, Li JY, Boado RJ, Pardridge WM. Organ-specific gene expression in the Rhesus monkey eye following intravenous non-viral gene transfer. Mol Vis 2003;9:465–72.

36. Luo X, Gong X, Tang CK. Suppression of EGFRvIII-mediated proliferation and tumorigenesis of breast cancer cells by ribozyme. Int J Cancer 2003;104:716–21.